HHS Public Access

Author manuscript

Nat Methods. Author manuscript; available in PMC 2015 December 01.

Published in final edited form as:

Nat Methods. 2015 November ; 12(11): 1051–1054. doi:10.1038/nmeth.3580.

Cas9 gRNA engineering for genome editing, activation and repression

Samira Kiani[1,2,11], **Alejandro Chavez**[3,4,5,11], **Marcelle Tuttle**[3], **Richard N Hall**[1,2], **Raj Chari**[5], **Dmitry Ter-Ovanesyan**[3,5], **Jason Qian**[3,5], **Benjamin W Pruitt**[3], **Jacob Beal**[6], **Suhani Vora**[1,3,5], **Joanna Buchthal**[3], **Emma J K Kowal**[3], **Mohammad R Ebrahimkhani**[1,7], **James J Collins**[1,2,3,8,9,10], **Ron Weiss**[1,2,7], and **George Church**[3,5]

[1]Department of Biological Engineering, Massachusetts Institute of Technology, Cambridge, Massachusetts, USA

[2]Synthetic Biology Center, Massachusetts Institute of Technology, Cambridge, Massachusetts, USA

[3]Wyss Institute for Biologically Inspired Engineering, Harvard University, Cambridge, Massachusetts, USA

[4]Department of Pathology, Massachusetts General Hospital, Boston, Massachusetts, USA

[5]Department of Genetics, Harvard Medical School, Boston, Massachusetts, USA

[6]Raytheon BBN Technologies, Cambridge, Massachusetts, USA

[7]Center for Emergent Behaviors of Integrated Cellular Systems (EBICS), Massachusetts Institute of Technology, Cambridge, Massachusetts, USA

[8]Institute for Medical Engineering & Science, Massachusetts Institute of Technology, Cambridge, Massachusetts, USA

[9]Broad Institute of MIT and Harvard, Cambridge, Massachusetts, USA

[10]Harvard-MIT Program in Health Sciences and Technology, Cambridge, Massachusetts, USA

Abstract

We demonstrate that by altering the length of Cas9-associated guide RNA(gRNA) we were able to control Cas9 nuclease activity and simultaneously perform genome editing and transcriptional

Correspondence should be addressed to R.W. (rweiss@mit.edu) or G.C. (gchurch@genetics.med.harvard.edu).

[11]These authors contributed equally to this work.

Accession codes. Raw RNA sequencing data are available at the NCBI GEO database under accession number GSE70694.

Note: Any Supplementary Information and Source Data files are available in the online version of the paper.

AUTHOR CONTRIBUTIONS

S.K. and A.C. designed and performed experiments and analyzed data. M.T., R.N.H., R.C., D.T.-O. and J.Q. performed experiments and interpreted data. S.V. and B.W.P. developed tools and contributed expertise. E.J.K.K. contributed to the analysis of RNA-Seq data. J. Beal helped with the initial design of repression promoter constructs and analysis of data via the TASBE method. M.R.E. helped with the design of experiments and interpretation of data. J. Buchthal analyzed data. J.J.C., R.W. and G.C. supervised the study. A.C., S.K., M.T. and M.R.E. wrote the manuscript with the support of all the other authors.

COMPETING FINANCIAL INTERESTS

The authors declare competing financial interests: details are available in the online version of the paper.

regulation with a single Cas9 protein. We exploited these principles to engineer mammalian synthetic circuits with combined transcriptional regulation and kill functions governed by a single multifunctional Cas9 protein.

So far no method exists that allows switching between Cas9 nuclease–dependent and –independent functions with relative ease. The ability of a single Cas9 protein to perform genomic modifications while simultaneously modulating transcription would allow a user to gain control of two critical cell biomolecules, DNA and RNA. A tool that made this possible would be transformative for a variety of applications, such as therapeutic interventions, genetic screening and synthetic genetic circuits[1–4].

In its native form, Cas9 is directed to a specific DNA sequence by a short gRNA that contains 20 nucleotides (nt) complementary to its target. Truncated gRNAs, with 17-nt complementarity, have been shown to decrease undesired mutagenesis at some off-target sites without sacrificing on-target genome-editing efficiency[5]. In the same study, however, gRNAs containing ≤16 nt showed a drastic reduction in nuclease activity. Analogous to earlier experiments examining the effects of increasing numbers of mismatches in a gRNA[6], we hypothesized that the lack of DNA cleavage with 16-nt gRNA was due not to a lack of DNA binding but to an inability of Cas9 to cleave the target substrate after binding.

We targeted Cas9 and a set of truncated gRNAs to the promoter of a transiently transfected fluorescent reporter. In agreement with previous results, Cas9 showed robust levels of nuclease activity with both 20-nt and 18-nt gRNAs and a sharp loss of function with ≤16-nt gRNAs (Supplementary Fig. 1a). To determine whether the lack of DNA modification observed with ≤16-nt guides was due to attenuated Cas9 nuclease activity, we fused a potent transcriptional activator (VPR) to Cas9 (ref. 7). We then targeted the Cas9-VPR fusion product to the same fluorescent reporter and quantified the effect of gRNA length on activation. As expected, Cas9-VPR showed minimal activation when a 20-nt gRNA was used, but when the gRNA length was decreased, a corresponding increase in activation was observed, with maximal activation achieved with 16-nt or 14-nt gRNAs (Supplementary Fig. 1b). Cas9-VPR showed nuclease activity similar to that of wild-type Cas9 with 20-nt or 18-nt gRNAs, and it demonstrated reporter activation equivalent to that of a fusion between nuclease-null Cas9 and VPR (dCas9-VPR) when 16-nt or 14-nt gRNAs were used (Supplementary Fig. 1). To assess the generality of this approach, we tested the effects of shortened gRNAs using two other Cas9 orthologues[8] and observed a similar capacity of shortened gRNAs to inhibit nuclease activity while still allowing interaction with DNA (Supplementary Fig. 2).

We next sought to determine whether our gRNA engineering paradigm would enable us to modulate Cas9 activity at endogenous target genes. Using 20-, 16- and 14-nt gRNAs, we targeted Cas9, Cas9-VPR and dCas9-VPR to the promoter regions of genes encoding structural proteins (*ACTC1* and *TTN*), a long noncoding RNA (*MIAT*) and a protein critical to tissue oxygen delivery (*HBG1*). Cas9-VPR was able to induce target chromosomal gene expression with 16-nt and 14-nt gRNA, but not with 20-nt gRNA (Fig. 1a–c and Supplementary Fig. 3). In addition, Cas9-VPR in conjunction with a 14-nt gRNA was able to generate expression equivalent to at least 40% of the expression level for all targets tested

when compared with dCas9-VPR with a 20-nt gRNA. In addition to measuring gene induction, we also examined the amount of Cas9-induced insertions and deletions (indels) in the targeted regions. For *ACTC1* and *MIAT*, mutagenesis was observed only with 20-nt gRNAs (Fig. 1a,b), whereas for *TTN* and *HBG1*, indels were observed with both 20-nt and 16-nt gRNAs (Fig. 1c and Supplementary Fig. 3).

To further characterize 14- and 20-nt gRNAs, we generated a series of spacer-mismatched fluorescent reporter plasmids and performed genome-wide RNA sequencing (Supplementary Figs. 4 and 5). The results as a whole suggested that 14-nt gRNAs showed a decrease in mismatch tolerance and no significant increase in undesired off-target activity.

Having demonstrated an ability to modulate Cas9 nuclease activity by simply altering gRNA length, we set out to determine whether we could perform nuclease-independent and nuclease-dependent functions simultaneously in a population of cells with a single Cas9 protein. We introduced Cas9 or Cas9-VPR along with a series of 14-nt gRNAs to target *TTN* and *MIAT* for activation and 20-nt gRNAs to target *ACTC1* for mutation. Compared with wild-type Cas9, Cas9-VPR exhibited robust *TTN* and *MIAT* gene induction while also generating a similar level of genomic mutation at the *ACTC1* locus (Fig. 1d and Supplementary Fig. 6). As an extension of these experiments, we also found that by using aptamer-based gRNA tethering systems, we could endow Cas9 in cell lines and organisms already expressing the protein with the ability to concurrently cut and activate a set of targets (Supplementary Fig. 7).

Next, we generated a number of synthetic transcriptional devices and layered circuits in human cells using the multifunctional CRISPR (clustered, regularly interspaced, short palindromic repeats)–multifunctional Cas9 protein system to test the utility of such a system for synthetic biology purposes. We first developed a library of our previously described CRISPR-repressible promoters (CRPs)[9] to identify promoter architectures that allowed us to achieve efficient Cas9-VPR–mediated transcriptional repression (Supplementary Figs. 8 and 9). We then performed a parallel experiment using the high-performance member of this promoter library (CRP-8, referred to as CRP-a in subsequent experiments) and confirmed similar repression efficiency (approximately tenfold repression) using dCas9 or Cas9-VPR with a 14-nt gRNA to this promoter (Fig. 2a).

We then evaluated the use of Cas9-VPR and 14-nt gRNAs in a single cell to achieve simultaneous transcriptional activation and repression. A CRP was placed upstream of enhanced yellow fluorescent protein (EYFP), and a CRISPR-activatable promoter (CAP) was placed upstream of tdTomato fluorescent protein. We transfected HEK293FT cells with both promoters, along with other circuit regulatory elements. Flow cytometry analysis 48 h after transfection showed that simultaneous repression and activation of the fluorescent reporters (~15-fold) were achieved with two 14-nt gRNAs that targeted Cas9-VPR to the two promoters (Fig. 2b and Supplementary Fig. 8b).

Subsequently, we designed a genetic kill switch in which a 20-nt gRNA that cut within a CAP was expressed under a tetracycline response element (TRE) promoter[9,10]. In the absence of a small-molecule inducer (doxycycline), Cas9-VPR in combination with

constitutively expressed 14-nt gRNA for the same target in the CAP activated expression of EYFP. After the addition of doxycycline, the 20-nt guide enabled Cas9-VPR to bind and cut within the CAP, leading to decreased EYFP expression (Fig. 2c and Supplementary Fig. 8c). When a similar circuit was used in which Cas9-VPR was replaced with dCas9-VPR, doxycycline addition led to an increase rather than a decrease in EYFP expression (Fig. 2c). Further analysis of this circuit revealed the dynamics and dosage response within this circuit topology (Supplementary Note 1 and Supplementary Figs. 10 and 11).

We then tested a genetic kill-switch design that operated by modulating the availability of Cas9-VPR in a cell. In our circuit, in the presence of a pair of full-length 20-nt gRNAs targeting the middle of the Cas9-VPR coding sequence, the guides directed Cas9-VPR to cut and disable itself and, by doing so, decreased the available pool of Cas9-VPR in the cell, ultimately causing a decrease in Cas9-VPR– and 14-nt gRNA–mediated inhibition and activation of the two fluorescent reporters (Supplementary Fig. 12).

Next, we developed and analyzed progressively complex genetic kill switches that ultimately incorporated the three discussed functions of a single Cas9-VPR protein. To this end, we used one of our previously characterized transcription activator–like effector repressors (TALERs)[11,12] and first tested whether Cas9-VPR could cleave within the TALER coding sequence and decrease the amount of available TALER, thereby negating its repression of EYFP (Supplementary Fig. 13). We then generated a modified U6 promoter[9] regulated by TALERs that enabled us to connect the genetic kill switch with a Cas9-VPR 14-nt gRNA repression device. Transfection of HEK293FT cells with this circuit led to repression of output EYFP upon the addition of input 20-nt gRNAs that cut within the TALER coding sequence (Supplementary Fig. 14). Finally, we combined and interconnected the genetic kill switch described in Supplementary Figure 14 with a Cas9-VPR–mediated transcriptional activation device to build a multilayered genetic circuit that simultaneously incorporated CRISPR-mediated transcriptional repression, activation and DNA cleavage in a single circuit to modulate the output (Fig. 2d and Supplementary Fig. 8d). Flow cytometry analysis 24 and 48 h after transfection of HEK293FT cells revealed a functional circuit regulated by the input 20-nt gRNA against TALER (Fig. 2d).

The ability of a single Cas9 protein to regulate RNA production while also maintaining the capacity to cleave DNA will be of great use in deciphering complex biological interactions and developing artificial genetic circuits. A promising use of our gRNA design principles will be in easily extending existing Cas9-based genome editing systems to concurrently modulate gene expression. This is particularly appealing in cases where considerable effort has been expended toward the generation of Cas9-expressing strains of mice or other labor-intensive and costly model systems[13,14]. Further, our data suggest that nuclease-positive Cas9 can be easily endowed with other previously described dCas9 activities[15,16] such as *in vivo* chromosomal tracking[17], and they could facilitate the development of multifunctional synthetic genetic safety circuits with potential biomedical applications.

ONLINE METHODS

Fluorescent reporter assay for quantifying Cas9 activation

Fluorescent reporter experiments described in Supplementary Figures 1 and 2 were conducted with a plasmid (Addgene, 47320) modified to include an extra gRNA binding site 100 bp upstream of the original one. For ST1 and SA Cas9 experiments, the protospacer remained the same but the PAM sequence was modified as needed for ST1 or SA Cas9. All experiments described in Supplementary Figure 4 were conducted with a reporter with a single gRNA binding site. Reporter 1 was Addgene 47320, and reporters 2 and 3 were similar to reporter 1 except that the protospacer and PAM (in bold) were changed to contain the sequences GGGGCCACTAGGGACAGGAT**TGG** and AAGAGAGACAGTACATGCCC**TGG**, respectively. HEK293T cells were cotransfected with gRNAs of various lengths, the indicated Cas9 protein and reporter and an EBFP2 transfection control. gRNA sequences for these experiments can be found in Supplementary Note 2. Cells were analyzed by flow cytometry 48 h after transfection and then, when necessary, were lysed for extraction of genomic DNA.

Reporter deletion analysis

DNA was extracted with QuickExtract DNA extraction solution (Epicentre). DNA was then used for PCR to amplify specific regions. PCR primers can be found in Supplementary Note 2. The amplified samples were then run on a 2% agarose gel stained with GelGreen (Biotium) and visualized using Gel Doc EZ (Bio-Rad). Band intensity was quantified using GelAnalyzer.

Quantitative RT-PCR analysis

Samples were lysed and RNA was extracted using the RNeasy Plus mini kit (Qiagen). cDNA was made using the iScript cDNA synthesis kit (Bio-Rad) with 500 ng of RNA. Kapa SYBR Fast universal 2× quantitative PCR (qPCR) master mix (Kapa Biosystems) was used for qPCR, with 0.5 μl of cDNA used for each reaction. Activation was analyzed with the CFX96 Real-Time PCR detection system (Bio-Rad). Gene expression levels were normalized to levels of *ACTB*. qPCR primers can be found in Supplementary Note 2.

Analysis of endogenous indels

DNA was extracted from 24-well plates using 350 μl of QuickExtract DNA extraction solution (Epicentre) according to the manufacturer's instructions. Amplicon library preparation was done with two PCRs. The first PCR was used to amplify from the genome and add appropriate barcodes and parts of adapters for Illumina sequencing. The second PCR extended the Illumina adapters. In the first PCR, 5 μL of extracted DNA was used as a template in a 100-μL Kapa HiFi PCR reaction run for 30 cycles. PCR products were then purified using a homemade solid-phase reversible-immobilization bead mixture and eluted in 50 μL of elution buffer. For the second PCR, 2 μL of the first-round PCR was used as a template in a 25-μL reaction, and PCRs were run for a total of nine cycles. PCR products were then run on an agarose gel, extracted and column purified. Equal amounts of each

sample were then pooled and sequenced on an Illumina MiSeq using the paired-end 150 MiSeq Nano kit. PCR primers for this analysis can be found in Supplementary Note 2.

We merged mate pair reads into single contigs using FLASH[18]. Each contig was then mapped to a custom reference representing the three amplicons with bwa mem[19]. SAM output files were then converted to BAM files, and pileup files were generated for each sample with SAMtools[20]. We then analyzed pileup files with custom Python scripts to determine observed mutation rates. Mutations were counted only if they spanned some portion of the sgRNA target site. In addition, base quality scores of ≥28 were required for any mutations to be called. To minimize the impact of sequencing errors, we excluded single base substitutions in this analysis.

RNA sequencing for quantifying activator specificity

For each sample, 200 ng of total RNA was polyA selected using a Dynabeads mRNA purification kit (Life Technologies). The RNA was then DNAse-treated with Turbo DNase (Life Technologies) and cleaned up with Agencourt RNAClean XP beads (Beckman Coulter). RNA-Seq libraries were made using the NEBNext Ultra RNA library prep kit for Illumina (New England BioLabs) according to the manufacturer's instructions with NEBNext multiplex oligos (New England BioLabs). Libraries were analyzed on a BioAnalyzer using a High Sensitivity DNA analysis kit (Agilent). Libraries were then quantified using a Kapa Library Quantification Kit (Kapa Biosystems) and pooled to a final concentration of 4 nM. Sequencing was performed on an Illumina NextSeq instrument with paired end reads. Reads were aligned to the hg19 UCSC Known Genes annotations using RSEM v1.2.1 (ref. 21) and were analyzed in Python and R. Differential gene-expression analysis was done using the Voom[22] and Limma[23] packages in R for all genes with ≥1 transcript per million mapped reads in each replicate, and a one-way within-subjects analysis of variance was performed on the number of differentially expressed genes for each condition to quantify off-target effects, where differential expression was defined by a Benjamini-Hochberg adjusted P value of <0.05 and fold change of >2 or <0.5.

Statistical analysis

All *t*-tests were performed via the GraphPad QuickCalcs website (http://graphpad.com/quickcalcs/ttest1/?Format=SEM; accessed June 2015). Raw data are provided in the Supplementary Data.

Cell culture for endogenous target mutation or activation or deletion reporter

HEK293T cells (a gift from P. Mali, UCSD, San Diego, California, USA) were cultivated in Dulbecco's modified Eagle's medium (DMEM) (Life Technologies) with 10% fetal bovine serum (FBS) (Life Technologies) and penicillin-streptomycin (Life Technologies). Incubator conditions were 37 °C and 5% CO_2. Cells were tested for mycoplasma yearly. Cells were seeded into 24-well plates at 50,000 cells per well and transfected with 200 ng of Cas9 construct, 10 ng of guide, 60 ng of reporter (for reporter experiments) and 25 ng of EBFP2 (for reporter experiments) with Lipofectamine 2000 (Life Technologies). After transfection, cells were grown for 48–72 h and lysed for either RNA or DNA extraction. gRNA for these experiments can be found in Supplementary Note 2.

Cell culture for circuit experiments

Experiments were carried out in HEK293FT cells obtained from ATCC and maintained in DMEM (CellGro) supplemented with 10% FBS (PAA Laboratories), 1% l-glutamine–streptomycin–penicillin mix (CellGro) and 1% nonessential amino acids (HyClone) at 37 °C and 5% CO_2 and tested for mycoplasma contamination. Transfections were performed using Lipofectamine LTX and Attractene reagents (Qiagen). Cells were seeded the day before transfection at 2×10^5 cells per well in a 24-well plate. Dosages of plasmids used for the transfection of synthetic circuits are presented in Supplementary Note 3. In control experiments, we replaced the DNA plasmid under study with an equivalent amount of empty DNA plasmid to keep the total amount of transfected DNA constant among the groups. For transfections involving Attractene reagent, cocktails of plasmid DNAs were mixed and added to serum-free DMEM to a total volume of 70 µl. 1.5–2 µl of Attractene was then added to each tube of DNA-DMEM mixture, and tubes were gently mixed and kept at room temperature for 25 min to allow the DNA-liposome complex to form. For experiments involving Lipofectamine LTX, cocktails of plasmid DNAs, serum-free DMEM and the Plus reagent were mixed and incubated for 10 min. In parallel, LTX reagent was mixed with the serum-free media and incubated for the same period of time. After the 10-min incubation, the two reagents were mixed and incubated for an additional 30 min. Fresh medium was added to the cells directly before transfection (500 ml of DMEM with supplements). The DNA-reagent solution was then added dropwise to the wells. Induction of the circuit was performed at this time as well via the addition of doxycycline.

Vector design and construction

Reporter gRNA (Addgene, 48672), dCas9-VPR (Addgene, 63798) and Cas9 (Addgene, 41815) were described previously. Cas9-VPR was cloned via Gateway assembly (Invitrogen) based on the Cas9 plasmid. gRNAs for endogenous targets were cloned into Addgene 41817 and transiently transfected. Plasmids used for synthetic circuits were constructed using the Gateway system, and the sequences are provided in Supplementary Note 4. The U6-driven gRNA expression cassettes were ordered as gblocks from IDT and cloned into a plasmid backbone using Golden Gate cloning. The library of CRPs was ordered as gene fragments from IDT and assembled into an appropriate promoter entry vector. Cas9-VPR plasmids used in this study have been submitted to Addgene (68495, 68496, 68497 and 68498).

Flow cytometry for circuit experiments

Flow cytometry data were collected 48 h after transfection. Cells were trypsinized and centrifuged at 453*g* for 5 min at 4 °C. The supernatant was then removed, and the cells were resuspended in Hank's balanced salt solution without calcium or magnesium supplemented with 2.5% FBS. A BD LSR II was used to obtain flow cytometry measurements with the following settings: EBFP, measured with a 405-nm laser and a 450/50 filter; EYFP, measured with a 488-nm laser and a 530/30 filter; and tdTomato, measured with a 561-nm laser and a 695/40 filter. Nontransfected controls were included in each experiment. Sample sizes were predetermined for each experiment on the basis of initial pilot experiments. We

also ensured that we gathered at least 100,000 flow cytometry events per biological replicate. Raw data are provided in the Supplementary Data.

Statistical analysis for circuit experiments

Flow cytometry data were converted from arbitrary units to compensated molecules of equivalent fluorescein (MEFL)[24] using the Tool-Chain to Accelerate Synthetic Biological Engineering (TASBE) characterization[25] (http://web.mit.edu/jakebeal/www/Publications/MIT-CSAIL-TR-2012-008.pdf). In this process an affine compensation matrix is computed from single positive and blank controls. Measurements of FITC dye are calibrated to MEFL using SpheroTech RCP-30-5-A beads, and mappings from other channels to equivalent FITC are computed from cotransfection of constitutive blue, yellow and red fluorescent proteins, each controlled by the *CAG* promoter on its own otherwise identical plasmid. Nontransfected controls were included in each experiment in this study. Sample sizes were predetermined for each experiment. Data shown in the figures are the geometric mean and s.d. for cells expressing the transfection marker EBFP or mKate on the basis of the MEFL threshold set. More precisely, we selected a threshold as a cutoff for each data set on the basis of the observed constitutive fluorescence distributions and excluded data below that threshold for being too close to the nontransfected population. Then we divided MEFL data by constitutive fluorescent protein expression into logarithmic bins at ten bins per decade and calculated the geometric mean and variance for the data points in each bin. We removed the high outliers by excluding bins without at least 100 data points. In fact, we calculated both population and per-bin geometric statistics using this filtered set of data. Exclusion criteria for samples during flow cytometry analysis were as follows: samples containing less than 10% of the number of events or less than 10% of the fraction of successful transfections of the mode for the batch in which they were collected.

Code availability

Scripts for determining mutation rates are available upon request.

Reproducibility

Sample sizes for each experiment were chosen on the basis of an initial pilot experiment and were further guided by sample sizes in similar experiments and publications. No randomization or blinding was used in the course of our experiments. No data were excluded from analysis.

Supplementary Material

Refer to Web version on PubMed Central for supplementary material.

Acknowledgments

We thank K. Esvelt, J. Scheiman, J. Huh, J. Aach, M.K. Cromer, S. Haque, M. Tung and all the other members of the Church, Collins and Weiss labs for their assistance and insightful discussions. We also thank P. Mali at University of California San Diego (UCSD; San Diego, California, USA) for the HEK293T cells. The dSaCas9 plasmid was a generous gift from F.A. Ran, W.X. Yan and F. Zhang (Broad Institute–MIT, Boston, Massachusetts, USA). This work was supported by US National Institutes of Health National Human Genome Research Institute grant P50 HG005550, US Department of Energy grant DE-FG02-02ER63445, the Wyss Institute for Biologically

Inspired Engineering, the US Army Research Office (DARPA W911NF-11-2-0054), the National Science Foundation (Emerging Frontiers in Research and Innovation Award in Engineering New Technologies Based on Multicellular and Inter-kingdom Signaling) and US National Institutes of Health grants 5R01CA155320-04 and P50 GM098792. A.C. acknowledges funding by the National Cancer Institute (grant 5T32CA009216-34). S.V. acknowledges funding by the National Science Foundation Graduate Research Fellowship Program, the Department of Biological Engineering at MIT and the Department of Genetics at Harvard Medical School. R.C. was funded by a Banting postdoctoral fellowship from the Canadian Institutes of Health Research. J.J.C. acknowledges funding from Defense Threat Reduction Agency grant HDTRA1-14-1-0006.

References

1. Hsu PD, Lander ES, Zhang F. Cell. 2014; 157:1262–1278. [PubMed: 24906146]
2. Sander JD, Joung JK. Nat. Biotechnol. 2014; 32:347–355. [PubMed: 24584096]
3. Qi LS, et al. Cell. 2013; 152:1173–1183. [PubMed: 23452860]
4. Mali P, Esvelt KM, Church GM. Nat. Methods. 2013; 10:957–963. [PubMed: 24076990]
5. Fu Y, Sander JD, Reyon D, Cascio VM, Joung JK. Nat. Biotechnol. 2014; 32:279–284. [PubMed: 24463574]
6. Jiang W, Bikard D, Cox D, Zhang F, Marraffini LA. Nat. Biotechnol. 2013; 31:233–239. [PubMed: 23360965]
7. Chavez A, et al. Nat. Methods. 2015; 12:326–328. [PubMed: 25730490]
8. Esvelt KM, et al. Nat. Methods. 2013; 10:1116–1121. [PubMed: 24076762]
9. Kiani S, et al. Nat. Methods. 2014; 11:723–726. [PubMed: 24797424]
10. Nissim L, Perli SD, Fridkin A, Perez-Pinera P, Lu TK. Mol. Cell. 2014; 54:698–710. [PubMed: 24837679]
11. Li Y, et al. Nat. Chem. Biol. 2015; 11:207–213. [PubMed: 25643171]
12. Davidsohn N, et al. ACS Synth. Biol. 2015; 4:673–681. [PubMed: 25369267]
13. Dow LE, et al. Nat. Biotechnol. 2015; 33:390–394. [PubMed: 25690852]
14. Platt RJ, et al. Cell. 2014; 159:440–455. [PubMed: 25263330]
15. Perez-Pinera P, et al. Nat. Methods. 2013; 10:973–976. [PubMed: 23892895]
16. Maeder ML, et al. Nat. Methods. 2013; 10:977–979. [PubMed: 23892898]
17. Chen B, et al. Cell. 2013; 155:1479–1491. [PubMed: 24360272]

References

18. Magoč T, Salzberg SL. Bioinformatics. 2011; 27:2957–2963. [PubMed: 21903629]
19. Li H, Durbin R. Bioinformatics. 2009; 25:1754–1760. [PubMed: 19451168]
20. Li H, et al. Bioinformatics. 2009; 25:2078–2079. [PubMed: 19505943]
21. Li B, Dewey CN. BMC Bioinformatics. 2011; 12:323. [PubMed: 21816040]
22. Law CW, Chen Y, Shi W, Smyth GK. Genome Biol. 2014; 15:R29. [PubMed: 24485249]
23. Smyth GK. Stat. Appl. Genet. Mol. Biol. 2004; 3 Article3.
24. Hoffman RA, Wang L, Bigos M, Nolan JP. Cytometry Part A. 2012; 81:785–796.
25. Beal J. Front. Bioeng. Biotechnol. 2015; 2:87. [PubMed: 25654077]

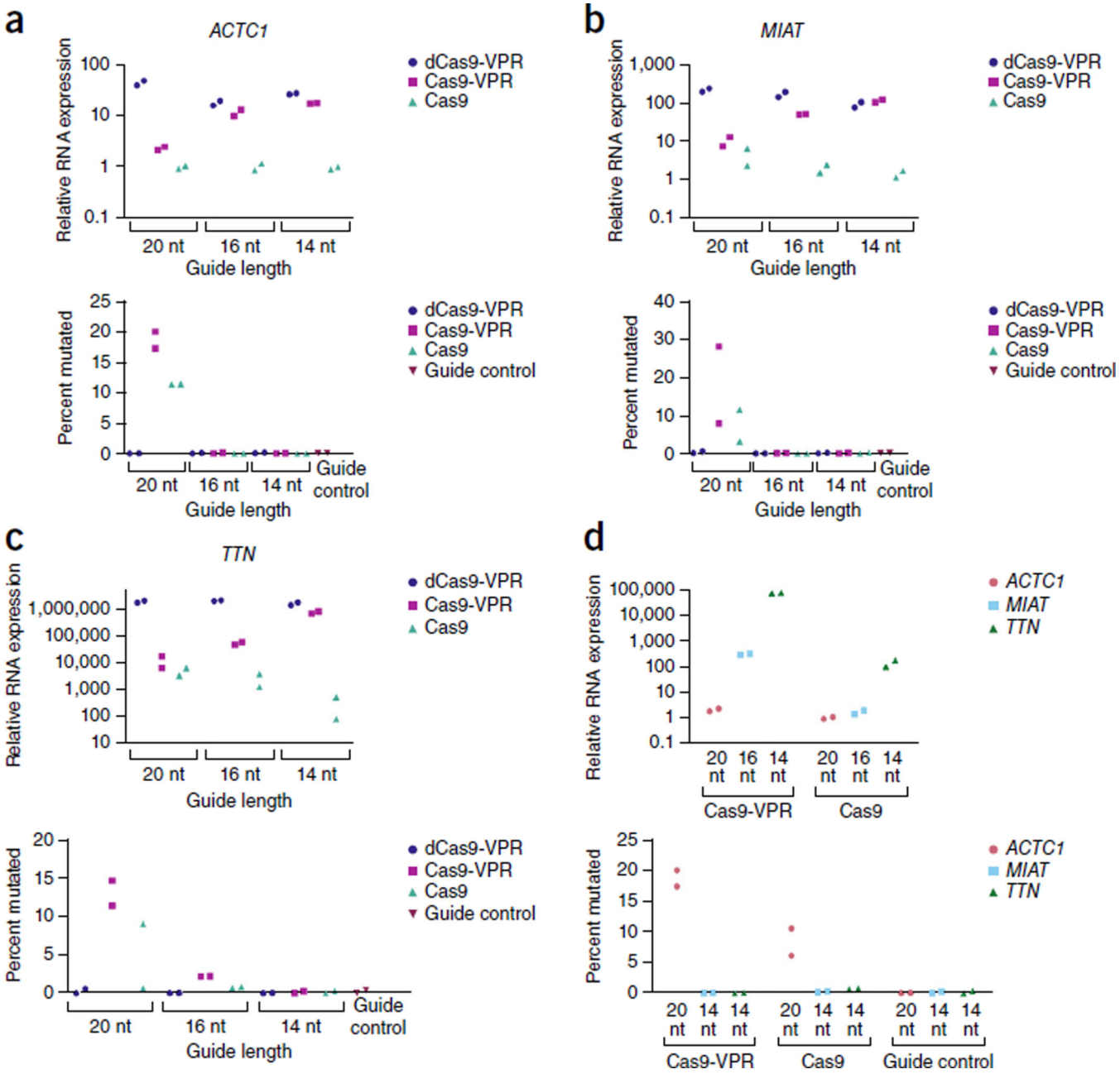

Figure 1.

Activation and cutting of endogenous genes in HEK293T cells. (**a–c**) RNA expression and mutagenesis analysis of the genes *ACTC1* (**a**), *MIAT* (**b**) and *TTN* (**c**). Each sample was transfected with the indicated Cas9 construct and gRNA of a particular length. Points represent data from two individual transfections. (**d**) Multiplexed activation and cutting of *ACTC1*, *MIAT* and *TTN*. The constructs were transfected with 20-nt *ACTC1* gRNA and 14-nt *MIAT* and *TTN* gRNAs simultaneously. Points represent data from two individual transfections.

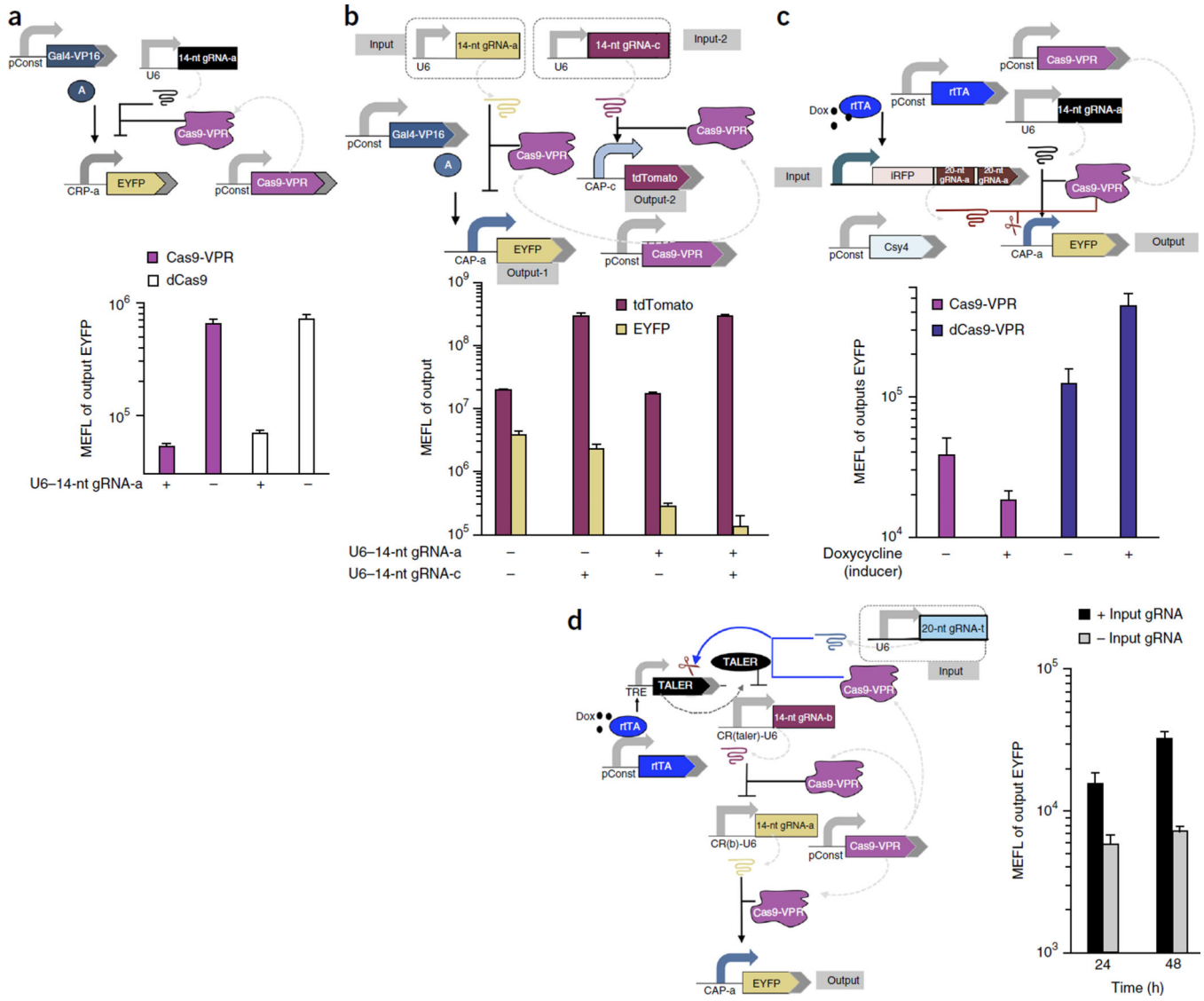

Figure 2.

Design and experimental analysis of human cells with multifunctional CRISPR devices and circuits. (**a**) Top, schematic of a repression device using Cas9-VPR and 14-nt gRNA. Bottom, the geometric mean and s.d. of EYFP expression for cells expressing >10^7 molecules of equivalent fluorescein (MEFL) of transfection marker enhanced blue fluorescent protein (EBFP). n = 3 independent technical replicates from three experiments (n = 2 for Cas9-VPR + gRNA). (**b**) Top, schematic of parallel Cas9-VPR and14-nt gRNA–based transcriptional repression and activation devices in a single cell. Bottom, the geometric mean and s.d. of EYFP and tdTomato expression for cells expressing >10^7 MEFL of transfection marker EBFP. n = 4 independent technical replicates combined from three experiments. (**c**) Top, schematic of a genetic kill switch designed to incorporate Cas9-VPR DNA cleavage and transcriptional activation functions. Bottom, the geometric mean and s.d. of EYFP expression for cells expressing >3 × 10^7 MEFL of transfection marker EBFP. n = 3 independent technical replicates from three experiments (n = 2 for Cas9-VPR without

doxycycline). rtTA, reverse tetracycline-controlled transactivator; iRFP, near-infrared fluorescent protein. (**d**) Left, genetic kill-switch circuit incorporating all three functions of Cas9-VPR: DNA cleavage, transcriptional activation and repression. Right, the geometric mean and s.d. of EYFP expression for cells expressing $>10^7$ MEFL of transfection marker mKate. $n = 4$ independent technical replicates from three experiments ($n = 2$ in 48-h groups). pConst, constitutively active promoter (e.g., CAG or hEF1-a).